



Heat transfer enhancement of TiO₂-water nanofluid flow in dimpled tube with twisted tape insert

S. Eiamsa-ard¹ · K. Wongcharee¹ · K. Kunrak¹ · Manoj Kumar² · V. Chuwattabakul³

Received: 26 December 2018 / Accepted: 8 April 2019 / Published online: 20 May 2019
© Springer-Verlag GmbH Germany, part of Springer Nature 2019

Abstract

This paper deals with the thermo-hydraulic behaviors of dimpled tubes mounted with twisted tape inserts using TiO₂-water nanofluids as the test fluids. The possible heat transfer mechanisms were discussed. Experiments were conducted using (1) the dimpled tubes with dimple angles (θ) of 0, 15, 30 and 45°, (2) the tapes having twist ratios (y/W) of 3.0, 4.0 and 5.0, and (3) TiO₂-water nanofluids with $\phi = 0.05, 0.1$ and 0.15 vol.%. The experimental results revealed that the dimpled tubes with twisted tapes yielded higher heat transfer rates than the dimpled tube alone. The results also indicated the strong influence of dimple angle, twist ratio and TiO₂-water nanofluid concentration on the thermo-hydraulic performance. Among the tested dimpled tubes, the one with a dimple angle of 45° yielded the highest heat transfer enhancement. Heat transfer (Nu) increased with decreasing twist ratio (y/W) and increasing nanofluid concentration. Over the investigated range, the highest thermo-hydraulic performance of 1.258 was achieved by using the nanofluid with $\phi = 0.15$ vol.% in the dimple angled having the dimple angle of 45°, inserted with twisted tape possessing the twist ratio of 3.0. In the present work, the Wilson plot method was employed to develop the Nusselt number correlation for the flow of TiO₂-water nanofluid through the dimpled tubes mounted with twisted tape inserts. The predicted heat transfer rate, friction factor and thermo-hydraulic performance were found in good agreement with the experimental results.

Nomenclature

A	Constant / heat transfer surface area, m ²
B	Constant
C	Constant

c_p	Specific heat capacity of fluid/nanofluid, J kg ⁻¹ K ⁻¹
d_i	Inside diameter, m
d	Diameter, m
f	Friction factor
h	Heat transfer coefficient, W m ⁻² K ⁻¹
k	Thermal conductivity of fluid/nanofluid, W m ⁻¹ K ⁻¹
L	Test section length, m
m	Constant
\dot{m}	Mass flow rate of fluid/nanofluid, kg s ⁻¹
Nu	Nusselt number
Q	Heat transfer rate of fluid/nanofluid, W
Re	Reynolds number
R_f	Fouling resistance, m ² K W ⁻¹
RTD	Resistance temperature detector
T	Temperature, K
ΔT_{LMTD}	Logarithmic mean temperature difference
U	Overall heat transfer coefficient, W m ⁻² K ⁻¹
V	Mean velocity inside the test section, m s ⁻¹
\dot{V}	Volume flow rate of fluid/nanofluid, m ³ s ⁻¹
W	Tape width, m
y	Tape twist length, m
y/W	Twist ratio

✉ S. Eiamsa-ard
smith@mut.ac.th

K. Wongcharee
khwanchi@mut.ac.th

K. Kunrak
kengkla.k@hotmail.com

Manoj Kumar
kmanoj1947@gmail.com

V. Chuwattabakul
kcvaresa@kmitl.ac.th

¹ Faculty of Engineering, Mahanakorn University of Technology, Bangkok 10530, Thailand

² Department of Mechanical Engineering, Faculty of Engineering, DIT University, Dehradun, Uttarakhand 248009, India

³ Faculty of Engineering, King Mongkut's Institute of Technology Ladkrabang, Bangkok, Thailand

ΔP Pressure drop, Pa

Greek symbols

ρ Density of the fluid/nanofluid, kg m^{-3}

μ Dynamic viscosity of the fluid/nanofluid, Ns m^{-2}

η Thermo-hydraulic performance

ϕ Concentration of nanofluid, % by volume

θ Dimple angle, $^\circ$

Subscripts

ave Average

c Cold fluid

E Enhanced device

h Hot fluid

i Inner tube

in Inlet

nf Nanofluid

np Nanoparticle

o Outer tube

out Outlet

0 Smooth/plain tube

p Particle

w Water

1 Introduction

The need to achieve high thermo-hydraulic performance and compact heat exchangers have pushed many industries to find for new methods to promote heat transfer. Applying dimpled surface is a unique passive technique for heat transfer enhancement (HTE). In this regard, the dimpled surface has emerged as one way to increase thermo-hydraulic performance and minimize the thermal boundary layer thickness of the heat exchangers' surfaces. The enhanced surfaces creates rotating and/or secondary flows that also increases the effectiveness of heat transfer surface area. It interrupts thermal and velocity boundary layer development with increasing degrees of turbulence near the rough tube wall. This, in turn, increases the convective heat transfer coefficient (h) with a consequent increase in the pressure drop along the tube. The studies of heat transfer enhancement in dimpled tubes were early reported by Kalinin et al. [1] and Giovannini et al. [2]. Several investigators have reported that dimpled tubes are effective devices for augmenting the rate of heat transfer in heat exchangers, especially for shell-tube and concentric-tube heat exchangers [3–10]. Suresh et al. [10] studied the thermo-hydraulic behavior in a dimpled tube with CuO-water nanofluids having various concentrations of nanoparticles (0.1, 0.2 and 0.3% by volume). It was concluded the use of nanofluids together with the dimpled tube resulted in better heat transfer as compared to the use of water as a testing fluid. Chen et al. [11] investigated the thermo-hydraulic behavior in a dimpled tube and found that the heat transfer rate with dimpled tubes increased by 25 to 137% over a plain tube. Wang

et al. [12] studied the thermo-hydraulic behaviors in the dimpled tubes for both staggered and aligned arrangements. They reported that the dimpled tubes in aligned arrangement enhanced heat transfer rate and friction factor up to 22.7 and 25.9% as compared to those of a plain tube. Wang et al. [13] also studied the thermo-hydraulic behavior in an ellipsoidal dimpled tube. Their results indicated that ellipsoidal dimpled tubes provided 175% higher heat transfer rate than a smooth straight tube with the nearly 75% higher pressure loss. García et al. [14] investigated the effect of dimpled tubes on the heat transfer rates in laminar and turbulent flow regimes. It was also reported that corrugated and dimpled tubes provided superior thermo-hydraulic performance to coiled wire which was attributed the lower pressure drop for similar convective heat transfer coefficients (h) encountered at Reynolds numbers higher than 2000. Kim [15] studied the influences of the roughness geometries on thermo-hydraulic behavior to optimize the dimpled tube configuration and found that dimpled tubes gave better thermo-hydraulic performance than a tube with diamond-shaped roughness. Li et al. [16] examined the thermo-hydraulic performance of a dimpled tube in steady state single phase (liquid-to-liquid) fluid flow for Reynolds numbers ranging from 500 to 8000 and for a water/glycol solution with Re ranging from 150 to 2000. It was reported that dimples disturbed the boundary layers, generating secondary flows which increased turbulence. Li et al. [17] investigated the heat transfer rate and pressure drop in helically dimpled tubes. Their results showed that the protrusion of dimples changed the fluid flow pattern, which enhancing turbulence through flow interaction and originated secondary flow. The maximum and average heat transfer coefficients of the helically dimpled tube were 2.48 and 1.74 times of the plain tube, respectively. Sarmadian et al. [18] investigated condensation heat transfer in a helically dimpled tube using refrigerant R-600a as a working fluid. Their results showed that the heat transfer rate was increased up to two times greater than that of a smooth straight tube. Kumar et al. [19] carried out analyses of the influence of a dimpled rib on the thermo-hydraulic performance of a heat exchanger tube. The maximum thermo-hydraulic performance and heat transfer rate were 2.87 times 3.18 times that of a plain tube, respectively. Ganjbakhsh et al. [20] reported the effects of surface roughness of semicircular curved horizontal dimple tubes on heat transfer, friction coefficient and thermal performance. Their results showed that the dimpled tube had better thermal performance than that a smooth tube especially at the low Reynolds number. Xie et al. [21] studied the heat transfer and thermal performance of enhanced tube with cross ellipsoidal dimples. They observed that the cross ellipsoidal dimples induced the transverse and longitudinal dimples which caused the reattachment and periodic impingement flows that helped in improving thermal performance. Again, Xie et al. [22, 23] examined the heat transfer and thermal enhancement

performance of enhanced tube with dimples and protrusions [22] and enhanced tube with teardrop dimples [23]. They reported that the enhanced tube with dimples and protrusions yielded thermal enhancement performance up to 1.65 while the enhanced tube with teardrop dimples yielded performance up to 2.06. Aroonrat and Wongwises [24] studied the effect of dimpled depth on heat transfer enhancement, pressure loss and overall performance of dimpled tubes. Their results showed that the dimpled tube with the largest dimpled depth gave the highest heat transfer enhancement and pressure loss up to 83 and 892% over those of the smooth tube.

Recently, nanofluids were applied in dimpled tubes for further heat transfer enhancement. Kumar et al. [25] investigated the thermo-hydraulic behaviors in a square passage with rib shape protrusions using Al_2O_3 -water, CuO-water, and ZnO-water nanofluids as working fluids in turbulent flow regime ($4000 \leq Re \leq 18,000$). The effects of nanofluid concentration, stream wise distance, and protrusion height to cross-section diameter ratio on thermo-hydrodynamic behaviors were reported. It was observed that the thermal performance increased with the concentration and decreased with nanoparticle diameter. Akyürek et al. [26] studied thermo-hydraulic behaviors in a concentric tube heat exchanger with Al_2O_3 -water nanofluids as the test fluids and used wire coil inserts as a turbulence promoter. The effects of nanofluid concentration and the pitch ratio of the wire coils on the thermo-hydraulic behavior were also studied. It was reported that pressure loss and heat transfer rate increased with increasing nanofluid concentration and decreasing pitch ratio of the wire coils. Suresh et al. [27] investigated the convective heat transfer characteristics of helically dimpled tubes using CuO-water nanofluid as the testing fluid. It was found that the use of nanofluids in a dimpled tube resulted in obvious enhancement of heat transfer coefficient with an insignificant increase of pressure loss. Recently, the combined effects of the nanofluids and helical/tape inserts were examined [28–31] and their results showed that the compound technique could improve the heat transfer rate and reduce exergy loss.

The above review shows that of the uses dimpled tubes, twisted tapes and nanofluids are the promising methods for thermal enhancement. The results of the dimpled tube, nanofluid, twisted tape and combined heat transfer enhancement techniques reported in literature motivates the current study of heat transfer augmentation using dimpled tubes with a nanofluid and twisted tape as a compound technique. Dimpled surfaces were used to boost the blending of the fluids via formation of secondary flow nearby the trough of the dimpled surfaces, nanofluids were applied to improve the thermo-fluid properties and twisted tapes were employed to promote the swirling flow along the flow pass. Current study was performed to evaluate the thermo-hydraulic performance in a heat exchange with compound technique. The effects of (1) dimpled tubes with four dimple angles of 0, 15, 30 and

45°, (2) twisted tapes with twist ratios of 3.0, 4.0 and 5.0, and (3) TiO_2 -water nanofluids with volume concentrations of 0.05, 0.1 and 0.15 vol.%, on thermo-hydraulic performance were investigated. The study encompassed Reynolds numbers (Re) ranging from 5000 to 15,000. The heat transfer rate and friction factor as well as empirical correlations for the Nusselt number, friction factor and thermo-hydraulic performance were also developed and reported.

2 Dimpled tube and twisted tape

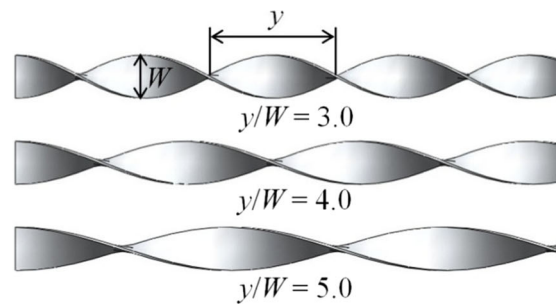
In the present work, concentric double pipe heat exchanger was employed. Inner tubes (dimpled tubes) were made of copper with an inner diameter of 18 mm while the annulus (smooth tube) was made of stainless steel with an inner diameter of 52 mm as displayed in Fig. 1. The dimpled tubes were fabricated with various dimple angles (θ) of 0, 15, 30 and 45°. The concentric tube heat exchanger with a length of 1100 mm was well insulated to minimize heat losses to environment. An image of the dimpled tube alone and dimpled tube with twisted tape inserted are shown in Figs. 1 and 2.

The dimpled surfaces were formed in a staggered manner, with a constant dimple pitch (p) = 12 mm or pitch ratio of $p/D = 0.67$. The diameter of an ellipsoidal dimple and its depth (e) were constant at $6 \times 3 \text{ mm}^2$ and 1.5 mm, respectively. Twisted tapes were inserted into dimpled tubes to generate swirls in the flow through the whole test section. Each twisted tape was formed from a stainless sheet with a thickness of 0.8 mm, length (L) of 1100 mm and width (W) of 15 mm. The twisted tapes used in the present study were fabricated with three twist lengths (γ) of 45, 60, and 75 mm, corresponding to twist ratios (γ/W) of 3.0, 4.0 and 5.0, respectively.

3 Experimental apparatus and methodology

A schematic diagram and photographs of the experimental setup for this heat transfer test are given in Figs. 3 and 4, respectively. The experimental apparatus consisted of a concentric tube heat exchanger, a set of resistance temperature detectors (RTDs) and T-type thermocouples, cooling and heating water batches, a differential pressure transducer, a mixer, centrifugal water pump, heater controller, a data logger, a personal computer and two rotameters to measure the volumetric flow rates of water as well as the nanofluids. The cold water flow was fed through a 2.0 m calming section to form a fully developed flow prior to being directed through the test section. A set of resistance temperature detectors (RTD) and T-type thermocouple sensors were utilized to measure bulk fluid and wall temperatures. Four RTDs were

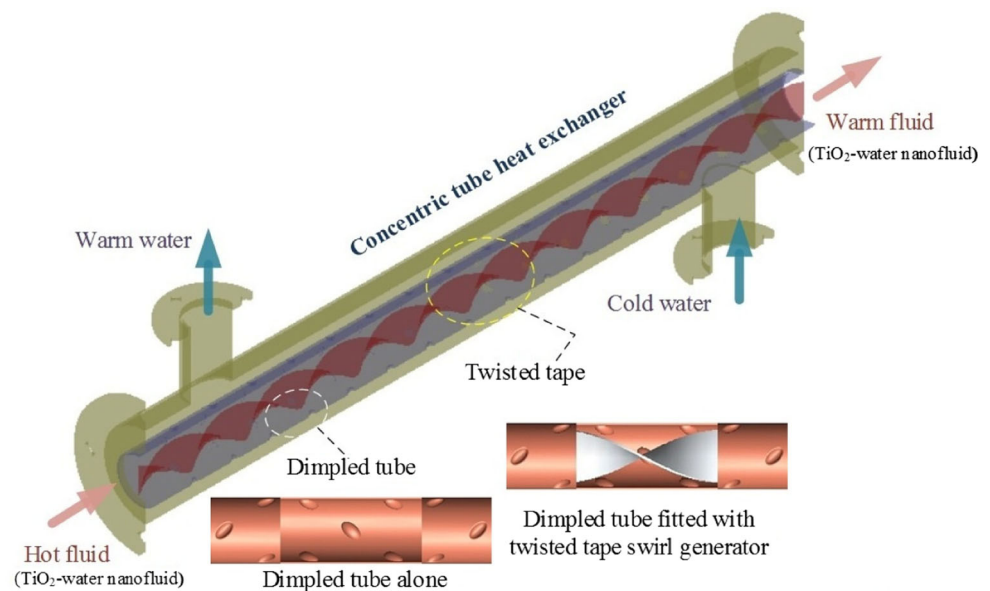
Fig. 1 Images of a dimpled tube and twisted tape inserts



(a) twisted tape with various twist ratios ($y/W = 3, 4$ and 5)



(b) dimpled tube inserted with twisted tape



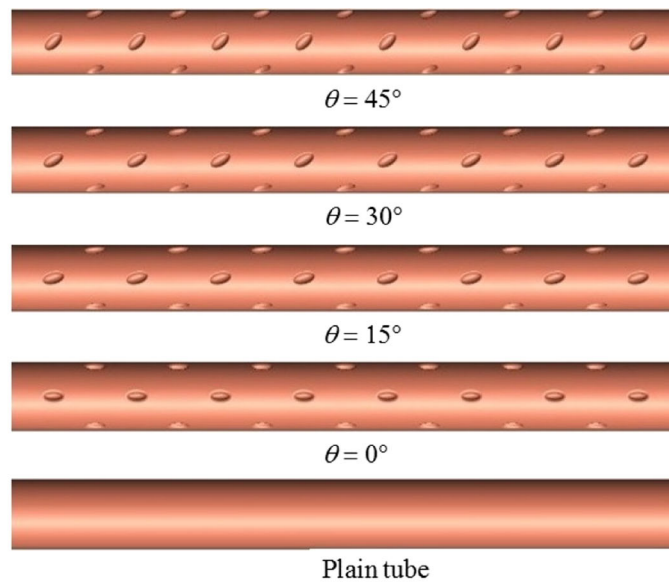
(c) concentric tube heat exchanger

mounted to measure the inlet and outlet water temperatures of the working fluids. During the experiments, a differential pressure transducer was used to monitor pressure loss (ΔP) of the fluids in the test section. The pressure loss across the test section was monitored under isothermal flow conditions (constant fluid temperature). Titanium dioxide (TiO_2) nanoparticles with an average diameter of 50 nm were purchased from Nanostructured and Amorphous Material, Inc., USA. Nanofluids were prepared with the required volume concentrations, 0.05, 0.1 and 0.15%, by dispersing the TiO_2 nanoparticles in de-ionized water. Then, the mixture was sonicated for 5 h prior to use as the working fluid.

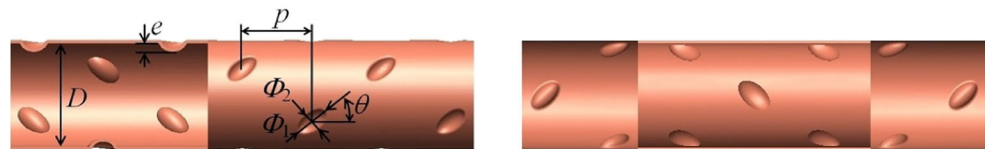
During experiments, hot fluids (water/nanofluids) flowed through the dimpled tube while cold water as a cooling medium flowed through the annulus of the counter-current flow heat exchanger. The temperature of inlet cooling water was kept constant at 25 °C and the flow rate of cold water was maintained at 500 l/h. The hot fluids were fed with the inlet temperature of 80 °C and Reynolds numbers ranging from 5000 to 15,000. All experimental data were recorded under steady state conditions.

The uncertainties of non-dimensional/dimensional parameters [32, 33] of the present experimental results are described in Table 1. The experimental results are within the reported uncertainty range.

Fig. 2 Images of plain tube and dimple tubes at various dimpled attach angles (θ)

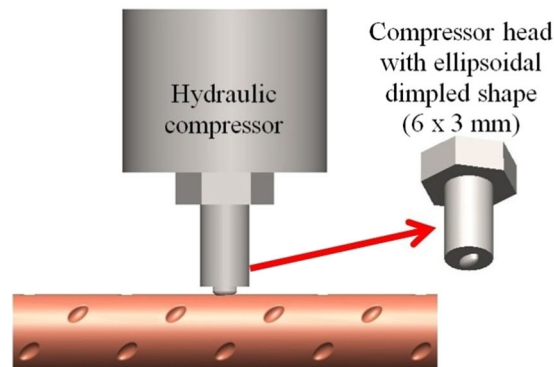


(a) plain tube and dimpled tubes



(b) outside dimpled tube

(c) inside dimpled tube



(d) forming of dimpled surface

4 Data reduction

4.1 Thermophysical properties of nanofluids

Thermophysical properties of nanofluids were evaluated using the widely used correlations which are mentioned below. The density of TiO_2 -water nanofluid (ρ_{nf}) was determined using the standard formula for the mixture:

$$\rho_{nf} = (1-\phi)\rho_w + \phi\rho_{np} \quad (1)$$

The specific heat ($c_{p,nf}$) of the TiO_2 -water nanofluid was determined by:

$$c_{p,nf} = \frac{\phi\rho_{np}c_{p,np} + (1-\phi)\rho_w c_{p,w}}{\rho_{nf}} \quad (2)$$

The above equations were found to be appropriate for TiO_2 -water nanofluid through equation below [34, 35]:

The thermal conductivity TiO_2 -water nanofluid (k_{nf}) was determined using Eq. (3).

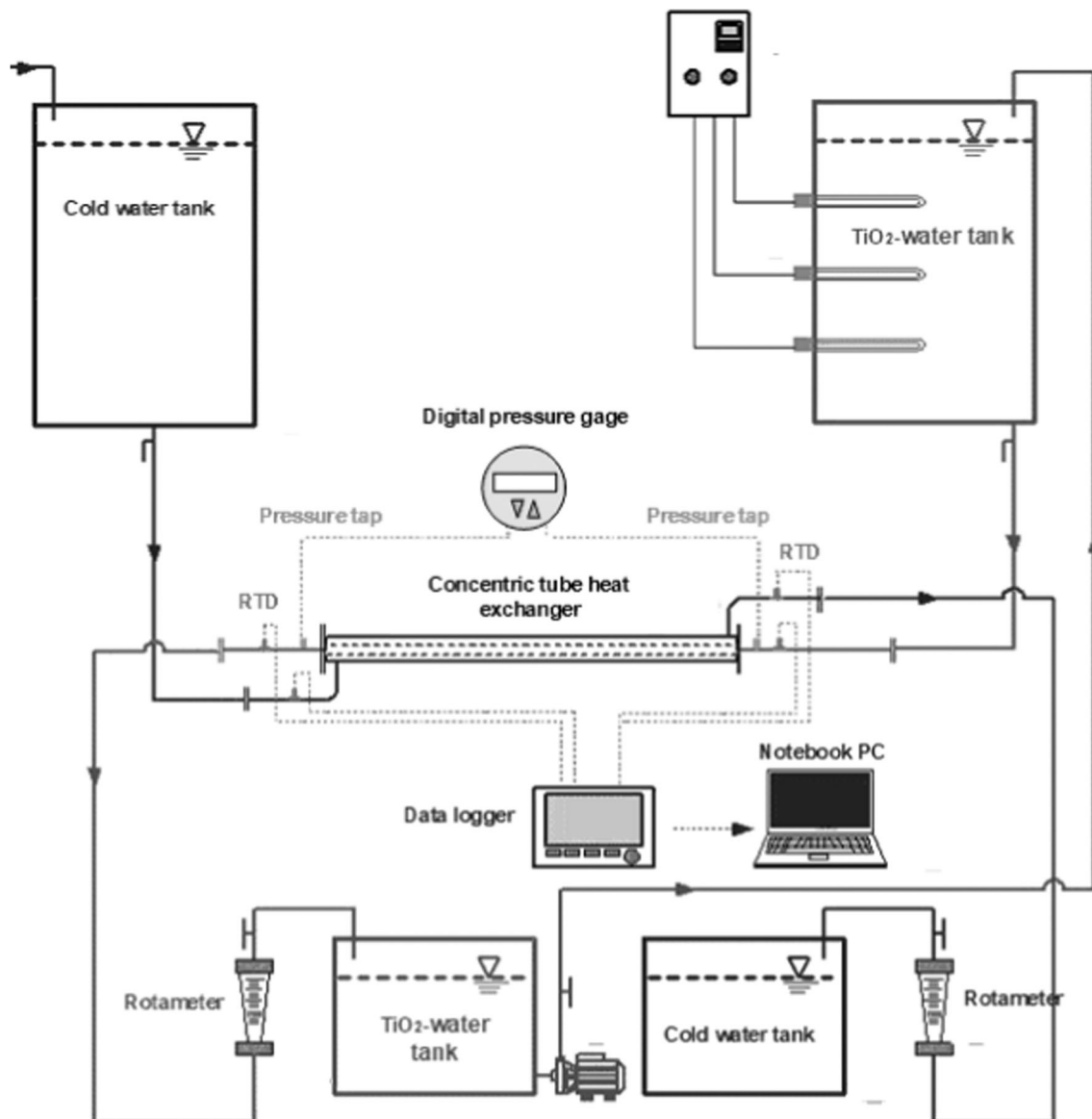


Fig. 3 Details of the experimental facility: (1) outer tube with PVC, (2) inner tube with plain copper tube or dimpled tube, (3–4) twisted tapes, (5) hot water tank, (6) electrical heater, (7) heater controller, (8) hot water pump, (9) rotameter for hot water, (10) resistance temperature detectors (RTDs), (11) U-tube manometer or digital pressure gage, (12) data logger, (13) personal computer, (14) water chiller for supplying cold water, (15) cold water pump and (16) rotameter for cold water

Fig. 4 Procedure of TiO₂-water nanofluid preparation

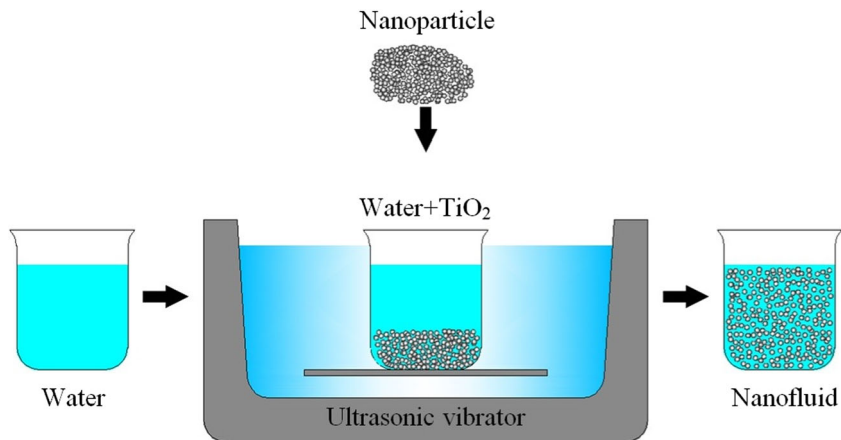


Table 1 Uncertainties of experimental parameters

Experimental parameter	Uncertainty
Inner tube diameter	±0.1 mm
Tube length	±0.1 mm
Temperature indicator (T , K)	±0.4%
Volumetric flow rate (V , m s ⁻³)	±3.4%
Pressure (P , Pa)	±1.5%
Friction factor (f)	±3.3%
Nusselt number (Nu)	±3.8%
Reynolds number (Re)	±3.1%

$$\frac{k_{nf}}{k_w} = \frac{k_{np} + 2k_w + 2\phi(k_{np} - k_w)}{k_{np} + 2k_w - \phi(k_{np} - k_w)} \quad (3)$$

The viscosity of TiO₂-water nanofluid (μ_{nf}) was evaluated using Einstein's formula expressed as:

$$\mu_{nf} = \mu_w(1 + \eta\phi) \quad (4)$$

4.2 Heat transfer, friction loss and thermo-hydraulic performance

In the experiments, the cold water absorbed heat from hot fluids flowing in the test section. The heat absorbed by the cold water and supplied by hot fluids were calculated from

$$\dot{Q}_c = \dot{m}_c c_{pc} (T_{c,out} - T_{c,in}) \quad (5)$$

$$\dot{Q}_h = \dot{m}_h c_{ph} (T_{h,out} - T_{h,in}) \quad (6)$$

where $\dot{m}_c = \rho_c \dot{V}_c$ and $\dot{m}_h = \rho_h \dot{V}_h$.

The cold and hot fluid flow rates, temperatures and the pressure losses in a dimpled tube were measured on both sides of the concentric tube heat exchanger using calibrated rotameters, resistance temperature detectors (RTD) and U-tube manometer or digital pressure gage. All the data were recorded and displayed on a personal computer (PC).

The mean heat transfer rates were given by:

$$Q_{ave} = (Q_c + Q_h)/2 \quad (7)$$

For fluid flows in a double pipe heat exchanger, the overall heat transfer coefficient (U) was determined from

$$Q_{ave} = UA_i \Delta T_{LMTD} \quad (8)$$

where

$$A_i = \pi d_i L \quad (9)$$

In the present work, the Wilson plot method was employed to develop the Nusselt number correlation for the flow of

TiO₂-water nanofluid through the dimpled tubes mounted with twisted tape inserts. The correlation development was based on the separation of the overall thermal resistance into the internal convective thermal resistance and the other thermal resistances involving the heat transfer process. In the experiments, the tube-wall temperature cannot be measured directly. Therefore, the tube-side convective heat transfer coefficient (h_i) was determined from the overall heat transfer coefficient (U) as found from Eqs. (8) and (9). The tube-side convective heat transfer coefficient (h_i) was evaluated as:

$$1/U = 1/h_i + A_i \ln(d_o/d_i)/2\pi kL + A_i/A_o h_o + R_f \quad (10)$$

Note that R_f is a fouling resistance [11]. When the last three terms ($A_i \ln(d_o/d_i)/2\pi kL$, $A_i/A_o h_o$ and R_f) on the right-hand side of Eq. (10) were kept constant and set to B , then Eq. (10) can be re-written as

$$1/U = 1/h_i + B \quad (11)$$

For the turbulent flow, the tube-side convective heat transfer coefficient (h_i) is proportional to the Reynolds number (Re) powered m that can be write in a function shown below [11]:

$$h_i = CRe^m \quad (12)$$

where C and m stand for constant and power index values.

Substituting Eq. (12) into Eq. (11) yields:

$$1/U = 1/CRe^m + B = A Re^{-m} + B \quad (13)$$

Equation (13) implies that the plot between $1/U$ and Re^{-m} is a straight line with its slope of A and intercept at B in Y -axis ($1/U$) [11]. Rearranging Eq. (13) yields

$$h_i = 1/(1/U - B) \quad (14)$$

The mean heat transfer rate (Nu) is then determined from

$$Nu = h_i d_H / k \quad (15)$$

The local thermal conductivity (k) of the fluid is determined from the fluid properties at the local mean bulk fluid temperature.

The Reynolds number (Re) is based on the flow rate at the inlet of the test section. The Reynolds number at the entry of the dimpled tube is

$$Re = \rho V d_H / \mu \quad (16)$$

where ρ and μ are the density and dynamic-viscosity of the test fluid and d_H is mean dimpled tube diameter.

The friction factor (f) in the dimpled tube can be calculated from

$$f = 2\Delta P d_H / (\rho L V^2) \quad (17)$$

Finally, the thermo-hydraulic performance can be written as [36, 37]:

$$\eta = \left(\frac{Nu_E}{Nu_0} \right) / \left(\frac{f_E}{f_0} \right)^{1/3} \quad (18)$$

To evaluate the thermal performance of the dimpled tube with enhance devices (twisted tape and nanofluid), the performance of the dimpled tube with enhance devices is evaluated relatively to the plain/smooth tube at an identical pumping power in the form of thermo-hydraulic performance (η).

5 Experimental results

The results of thermo-hydraulic behaviors showing the effects of (1) dimpled tubes with four dimple angles of 0, 15, 30 and 45°, (2) twisted tapes with twist ratios of 3.0, 4.0 and 5.0, and (3) TiO₂-water nanofluids with concentrations of 0.05, 0.1 and 0.15 vol.% are reported.

5.1 Validation test of a dimpled tube

Calibrated experimental test set-up was tested by using a conventional plain/smooth tube, for validation which is essential test to ensure the accuracy of the experimental data. The average Nusselt number and friction factor values were compared with the values calculated from the correlations developed by Dittus-Boelter and Gnielinski for Nusselt numbers (Nu) and Blasius and Petukhov correlations [38] for friction factors (f). The comparisons are presented in Fig. 5a–b. The Nusselt numbers obtained from the Dittus-Boelter and Gnielinski correlation were within ± 6.7 to $\pm 11.8\%$ of experimental values whereas the friction factors calculated from Blasius and Petukhov correlation were between ± 6.1 and $\pm 9.2\%$ of experimental data. The comparisons showed that the experimental data were within an acceptable range. Moreover, the experimental Nusselt numbers and friction factors data of the dimpled tube were also validated using published data [5, 13] as presented in Fig. 6a–b. The results of Thianpong et al. [5] and Wang et al. [13] results were comparable to the present experimental data and deviations within ± 3.6 and $\pm 10.5\%$ for Nusselt number and ± 50.6 and $\pm 48.5\%$ for friction factor.

5.2 Effect of dimpled angle (θ)

The influence of the dimple angles ($\theta = 0, 15, 30$ and 45°) on the heat transfer rate (Nu) of the dimpled tube inserted with a twisted tape insert is demonstrated in Fig. 7a. Evidently, heat transfer (Nu) increased significantly with increasing dimple angle since the rougher dimples cause stronger turbulence than the smoother ones. At a given Reynolds number, the highest Nusselt

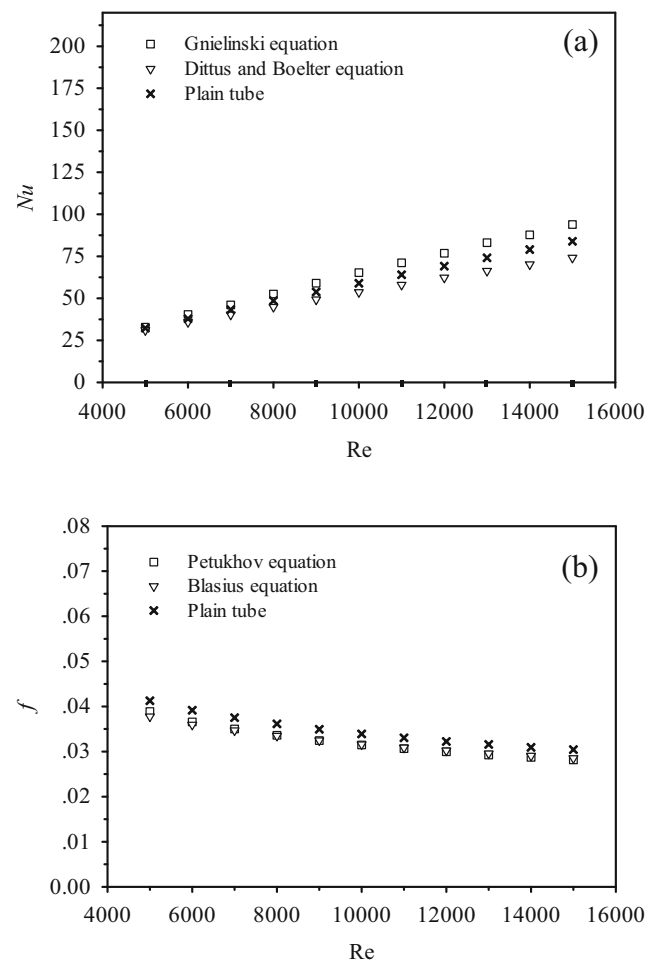


Fig. 5 Validation of the plain tube

number (Nu) was obtained by using the dimpled tube with the dimple angle of 45° . The heat transfer (Nu) of the dimpled tube with a 45° dimple angle was greater than that of tubes with dimple angles, 0, 15 and 30° , by 2.3, 1.6 and 0.7%, respectively. Figure 7b shows the Nusselt number enhancement ratio for dimple angles ranging from 0 to 45° . Nusselt number enhancement ratios ranged from 1.33 to 1.41 over the range of Reynolds numbers.

Figure 8a–b shows the effect of dimple angle on friction losses. It was found that friction loss and friction factor enhancement ratio increased with increasing dimple angle. At dimple angle of 45° , friction factor enhancement ratios ranged from 2.26 to 2.34, over the entire range of Re .

Figure 9 demonstrates the variation in the thermo-hydraulic performance ratio with Reynolds number at various dimple angles (0, 15 and 30°). Obviously, thermo-hydraulic performance ratio increased with increasing dimple angle, resulting from the better tradeoff between improved heat transfer and increased friction loss penalty. At dimple angle of 45° , thermo-hydraulic performance ratios ranged from 1.035 to 1.063, over the entire range of Re .

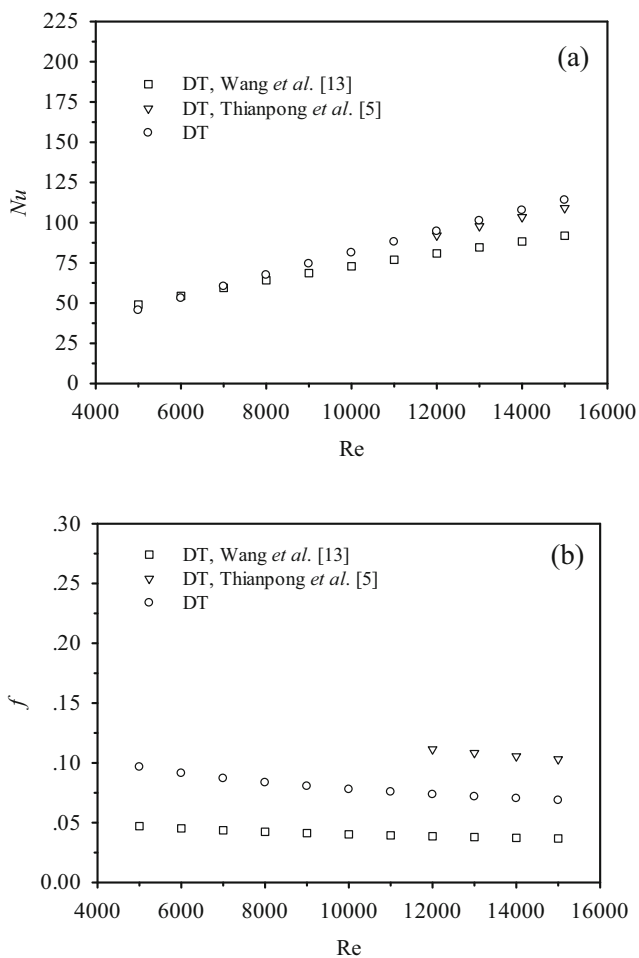


Fig. 6 Validation of the dimpled tube

5.3 Effect of twist ratio

The variation in the heat transfer rate (Nu) with Re for the dimpled tubes mounted with a twisted tape swirl generator (TT) is demonstrated in Fig. 10a–b. The heat transfer (Nu) of the plain tube is also reported for comparison. At comparable operating conditions, the heat transfer rate (Nu) of the dimpled tubes with TT s were consistently higher than those of the plain or the dimpled tubes alone, attributed to the combined effects of the turbulence/re-circulation flow induced by the dimpled rough surfaces and the swirling flow induced by TT s.

Figure 10a–b also reveals that Nusselt number and heat transfer enhancement ratio (Nu_E/Nu_0) increased as increasing dimpled angle of dimpled tubes and decreasing twist ratio of twist tapes. The mean Nusselt number (Nu) of the dimpled tube with twisted tape swirl generators having y/W of 3.0, 4.0 and 5.0 were higher than those of the dimpled tubes alone by 46.5, 39.2 and 32.7%, respectively, and higher than that of the plain tube alone by 106.9, 96.6 and 87.4%, respectively. In other words, the heat transfer enhanced by TT insert having y/W of 3.0 was higher than that promoted by TT s with y/W of 4.0 and 5.0 by 5.3 and 10.4%, respectively. It can be explained by the fact that the

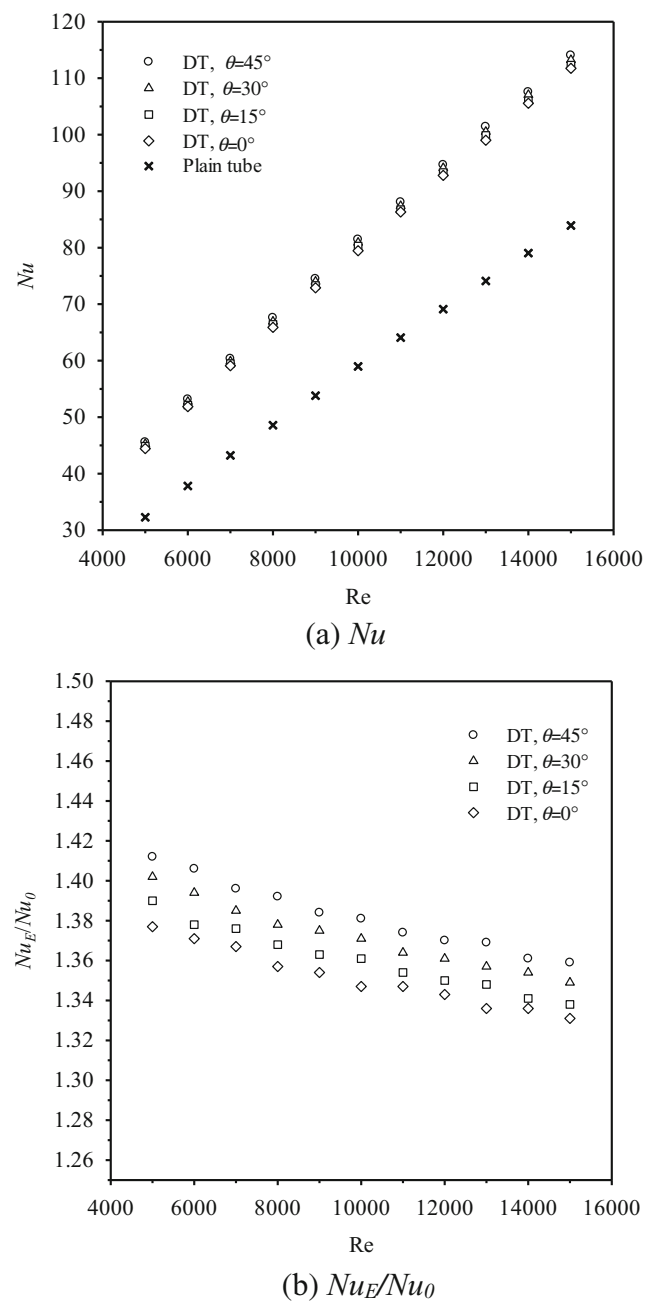
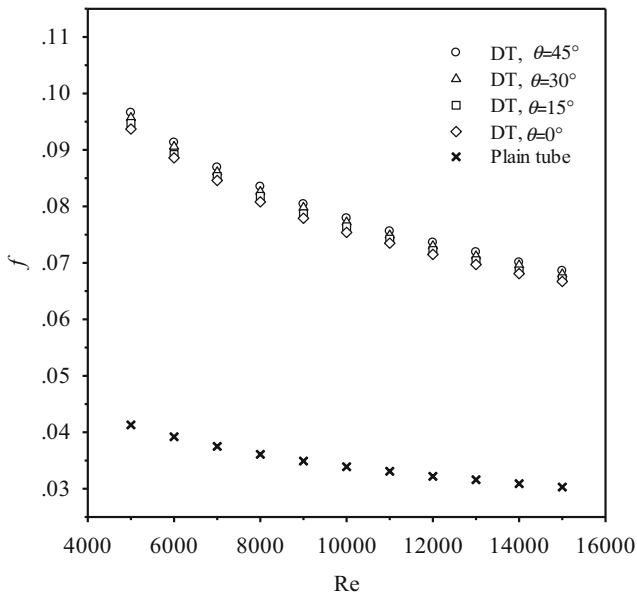


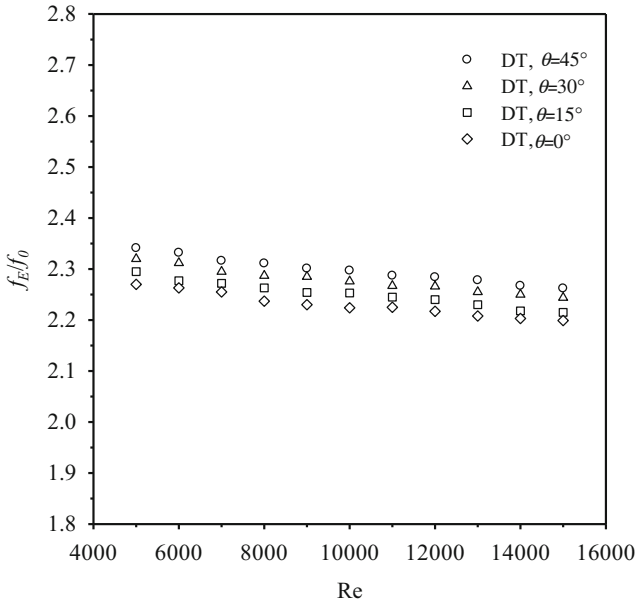
Fig. 7 Effect of dimple attach angle (θ) on the heat transfer rate

twisted tape with smaller y/W generates stronger swirl intensity which is more efficient in promoting fluid mixing, breaking the thermal boundary layer and thereby enhancing heat transfer.

The effect of the dimpled tubes combined with a TT insert on the friction factor (f) is displayed in Fig. 11a–b. It can be observed that friction factor (f) gradually increased with decreasing Reynolds numbers (Re). Under similar conditions, the friction factor (f) of the dimpled tubes mounted with TT insert caused higher friction factor (f) than the dimpled tubes alone and the plain tube due to (1) the larger surface area the dimple tube together with that of the twisted tapes and (2) the additional dissipation caused by the compound device. The



(a) f



(b) f_E/f_0

Fig. 8 Effect of dimple angle (θ) on the friction factor

friction factors of the dimpled tubes with twisted tape swirl generators were found to be 1.73–2.03 times over those of the dimpled tube alone and 3.96–4.69 times over those of the plain tube alone.

In Fig. 11a, shows that the maximum friction factor was caused by the compound device consisting of dimpled tube having the dimple angle of 45° and twisted tape having y/W of 3.0. The maximum friction factor was found to be higher than those caused in the dimpled tube with TTs having twist ratios of 4.0 and 5.0 by 7.8 and 16.0%, respectively. It was also found that the effects of dimple angle and twist ratio on

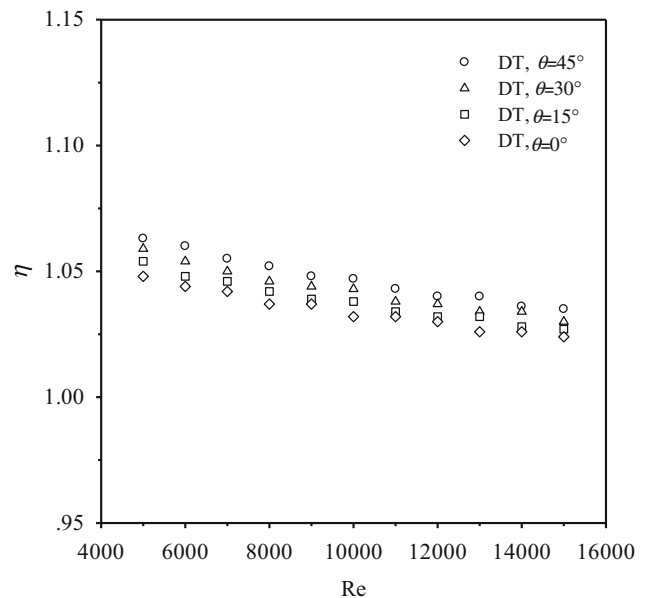
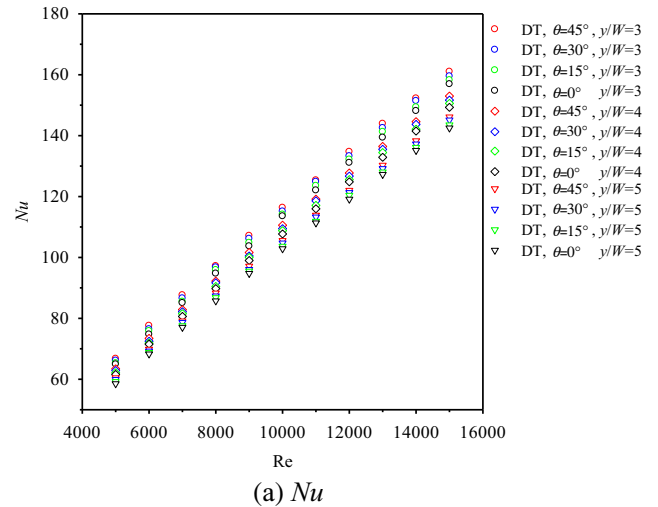
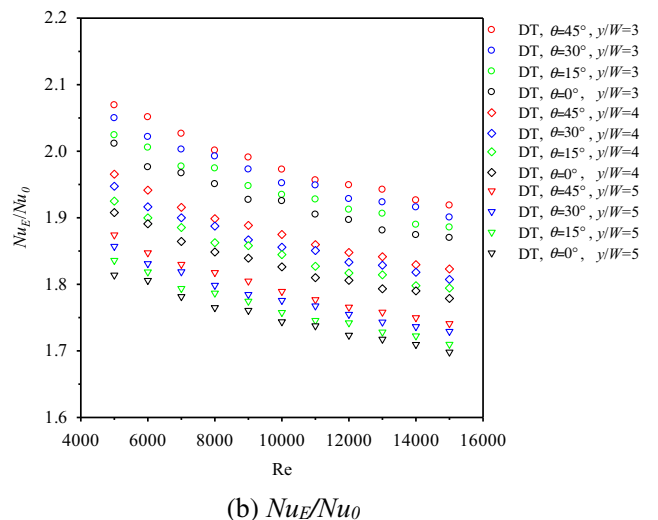


Fig. 9 Effect of dimple angle (θ) on the thermo-hydraulic performance



(a) Nu



(b) Nu_E/Nu_0

Fig. 10 Influence of twist ratio on heat transfer enhancement

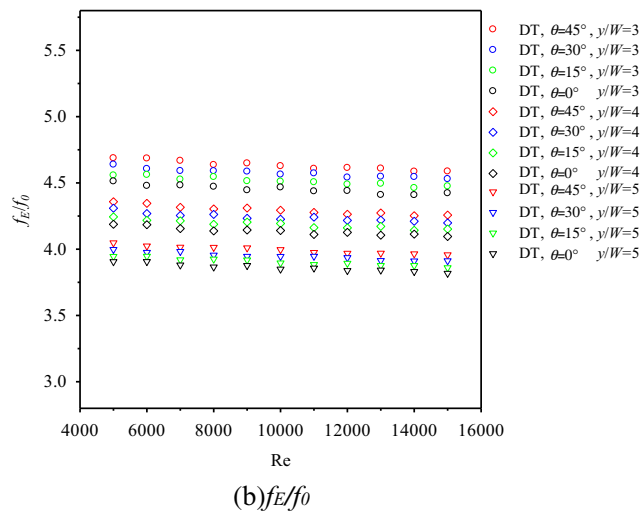
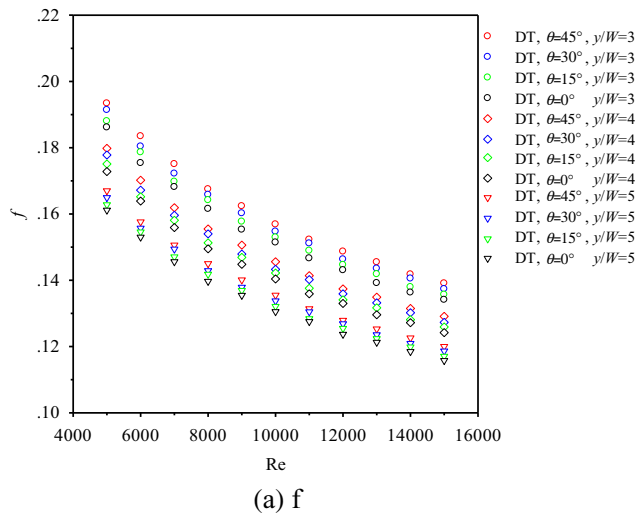


Fig. 11 Influence of twist ratio on friction factor

friction factor enhancement ratio are in similar manner with those on friction factor (Fig. 11b).

Figure 12 shows the influence of the twist ratio (y/W) on thermo-hydraulic performance. It was observed that the thermo-hydraulic performance increased with decreasing y/W . At Reynolds number of 5000, the highest thermo-hydraulic performance provided by the dimpled tubes combined with TT inserts having twist ratios of 3.0, 4.0 and 5.0 were 1.24, 1.20 and 1.18, respectively. In other words, the dimpled tube with the TT insert possessing twist ratio of 3.0 gave higher thermo-hydraulic performance than the identical tube with the TT inserts having twist ratios (y/W) of 4.0 and 5.0 by around 2.7 and 5.1%, respectively.

5.4 Effect of nanofluid concentration (ϕ)

Figures 13a–b, 14a–b and 15 show the effect of TiO_2 -water nanofluid concentration on heat transfer (Nu), friction loss and thermo-hydraulic performance of the dimpled tube with the

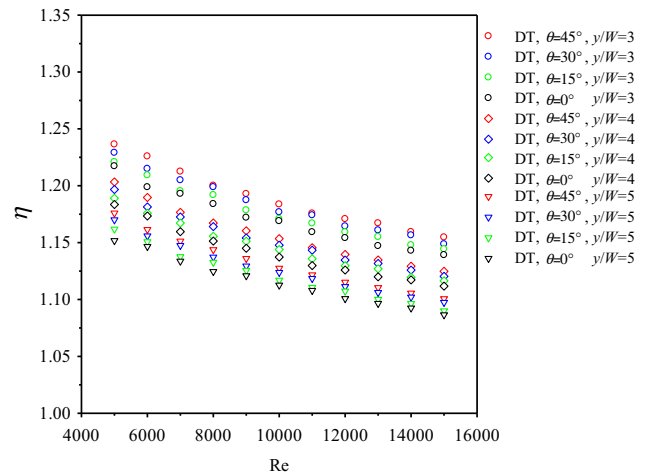


Fig. 12 Influence of twist ratio on the thermal performance

dimple angle of 45° . It was observed that heat transfer (Nu), friction loss and thermo-hydraulic performance increased as the TiO_2 -water nanofluid concentration increased. Over the investigated range, the highest thermo-hydraulic performance of

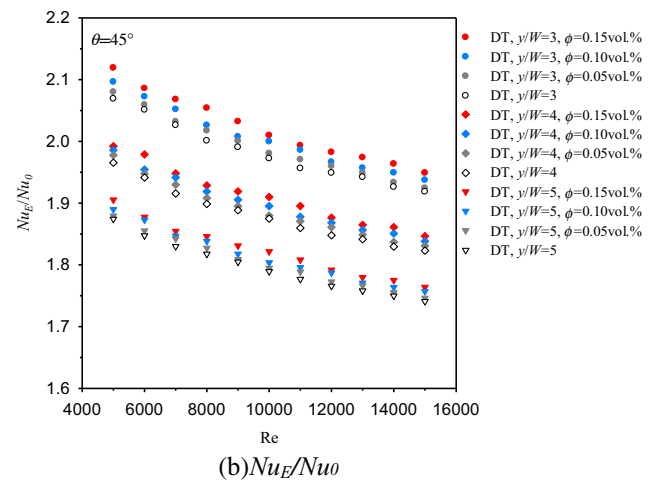
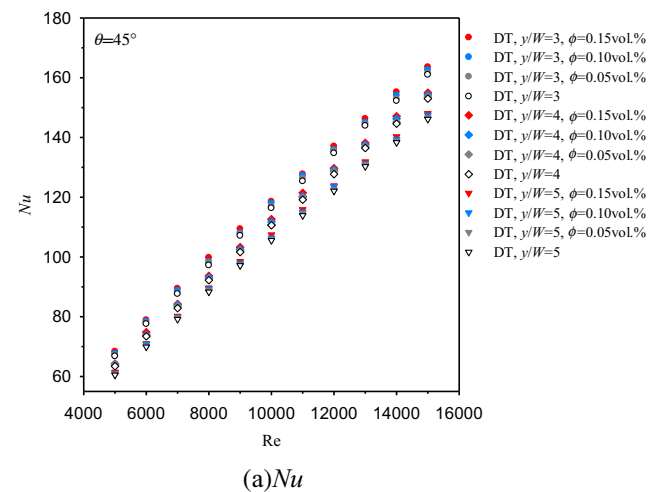


Fig. 13 Influence of nanofluid concentration (ϕ) on the heat transfer enhancement

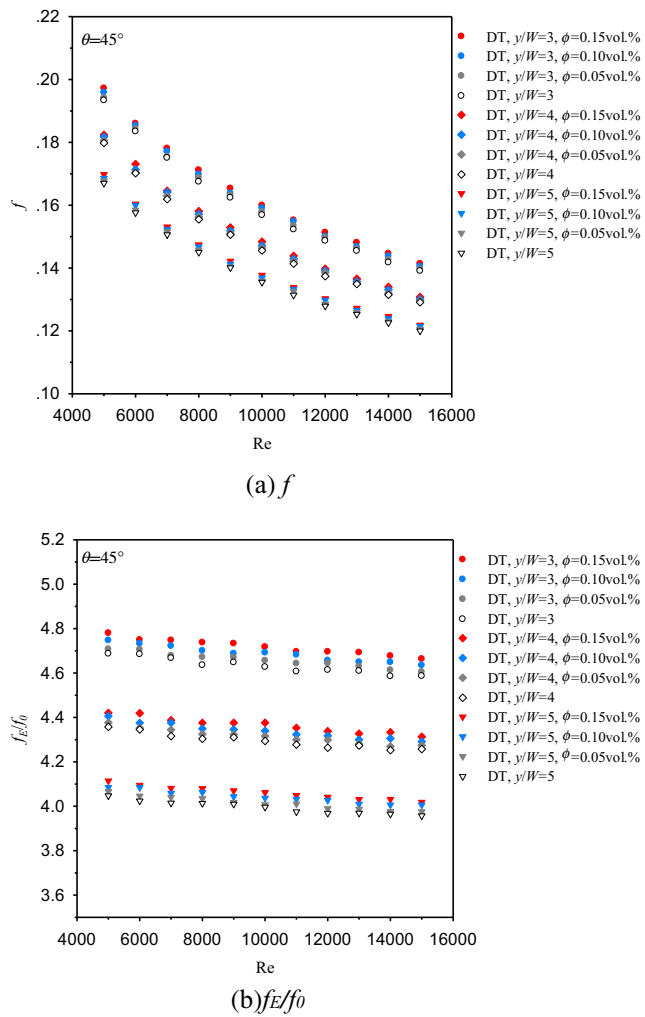


Fig. 14 Influence of nanofluid concentration (ϕ) on friction factor

1.258 was achieved by using the nanofluid with $\phi = 0.15$ vol.% in the dimple angled having the dimple angle of 45° , inserted with twisted tape possessing the twist ratio of 3.0.

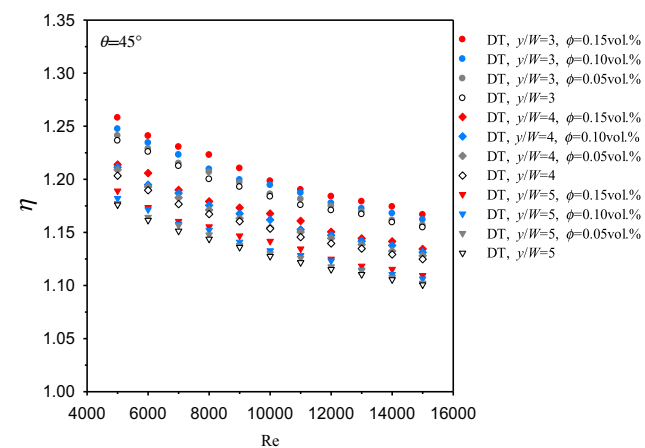


Fig. 15 Influence of nanofluid concentration (ϕ) on the thermal performance

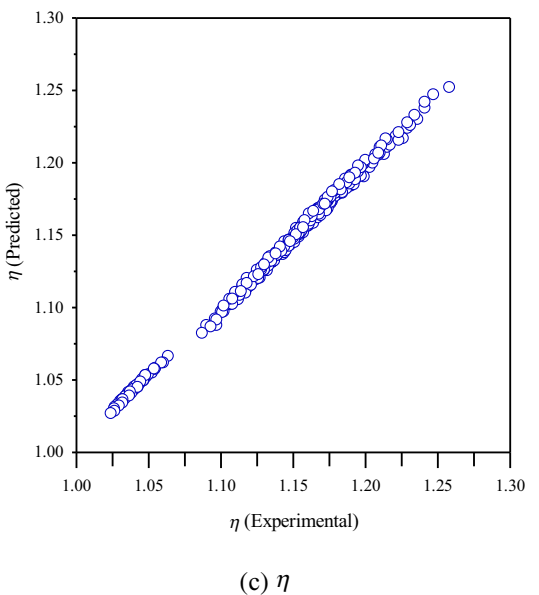
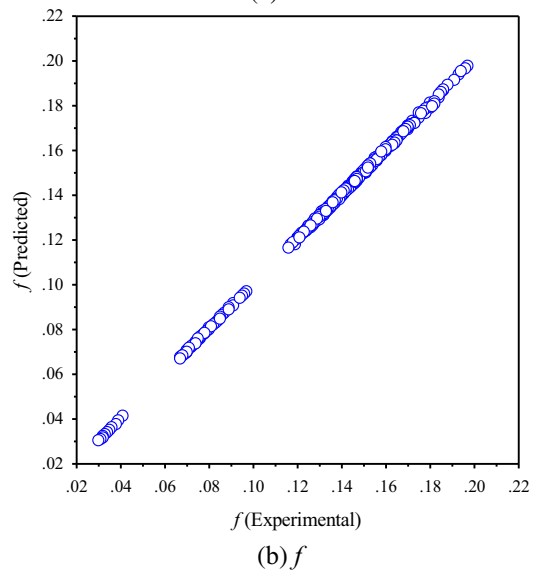
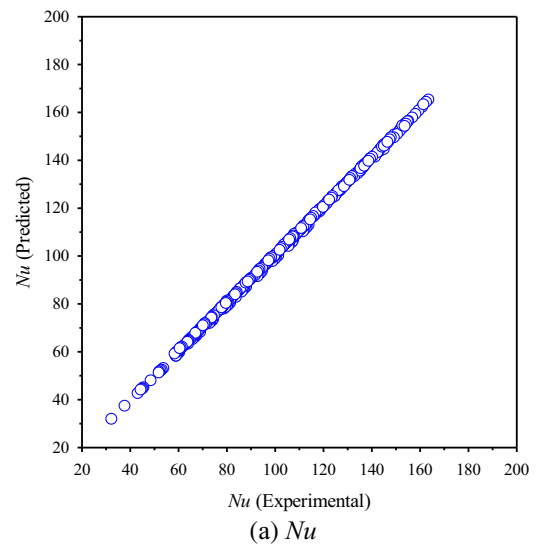


Fig. 16 Experimental data versus predicted data

5.5 Empirical correlation

Experimentally obtained data were used to develop correlations of Nu , f and thermo-hydraulic performance as function of flow Re , twist ratio and dimple angle using regression analysis. The Nu , f and thermo-hydraulic performance correlations for dimpled tube, dimpled tube with TT inserts and dimpled tubes containing TT inserts using a TiO_2 -water nanofluid are shown as follows:

Dimpled tube:

$$Nu_{DT} = 0.024Re^{0.836}Pr^{0.3}(1 + \tan\theta)^{0.034} \quad (19)$$

$$f_{DT} = 1.317Re^{-0.31}(1 + \tan\theta)^{0.044} \quad (20)$$

$$\eta_{DT} = 1.281Re^{-0.023}(1 + \tan\theta)^{0.018} \quad (21)$$

For $5000 \leq Re \leq 15,000$ and $0^\circ \leq \theta \leq 45^\circ$.

Dimpled tube inserted with twisted tape:

$$Nu_{DT-TT} = 0.057Re^{0.805}Pr^{0.3}(1 + \tan\theta)^{0.039}(y/W)^{-0.189} \quad (22)$$

$$f_{DT-TT} = 3.269Re^{-0.3}(1 + \tan\theta)^{0.054}(y/W)^{-0.28} \quad (23)$$

$$\eta_{DT-TT} = 2.224Re^{-0.059}(1 + \tan\theta)^{0.02}(y/W)^{-0.095} \quad (24)$$

For $5000 \leq Re \leq 15,000$, $0^\circ \leq \theta \leq 45^\circ$, and $3.0 \leq y/W \leq 5.0$.

Dimpled tube inserted with twisted tape and nanofluid:

$$Nu_{DT-TT-NF} = 0.062Re^{0.8}Pr^{0.3}(y/W)^{-0.197}(1 + \phi)^{0.135} \quad (25)$$

$$f_{DT-TT-NF} = 3.463Re^{-0.301}(y/W)^{-0.29}(1 + \phi)^{0.133} \quad (26)$$

$$\eta_{DT-TT-NF} = 2.36Re^{-0.063}(y/W)^{-0.1}(1 + \phi)^{0.09} \quad (27)$$

For $5000 \leq Re \leq 15,000$, $0^\circ \leq \theta \leq 45^\circ$, $3.0 \leq y/W \leq 5.0$, and $0.05 \text{ vol.\%} \leq \phi \leq 0.15 \text{ vol.\%}$.

Table 2 Summary of experimental results for dimpled tubes

Details	θ ($^\circ$, degree)	Nu_E/Nu_0	f_E/f_0	η
Dimpled tube	0	1.33–1.38	2.20–2.27	1.024–1.048
	15	1.34–1.39	2.21–2.30	1.027–1.054
	30	1.35–1.40	2.24–2.32	1.030–1.059
	45	1.36–1.41	2.26–2.34	1.035–1.063

Table 3 Summary of experimental results for dimpled tube with twisted tape inserts

Details	θ ($^\circ$, degree)	y/W	Nu_E/Nu_0	f_E/f_0	η
Dimpled tube	0	5.0	1.70–1.81	3.82–3.91	1.087–1.152
	0	4.0	1.78–1.91	4.10–4.19	1.112–1.184
	0	3.0	1.87–2.01	4.41–4.51	1.139–1.217
	15	5.0	1.71–1.84	3.86–3.95	1.090–1.162
	15	4.0	1.79–1.93	4.14–4.24	1.116–1.189
	15	3.0	1.89–2.02	4.46–4.56	1.144–1.221
	30	5.0	1.73–1.86	3.91–4.00	1.097–1.170
	30	4.0	1.81–1.95	4.20–4.31	1.120–1.197
	30	3.0	1.90–2.05	4.53–4.64	1.149–1.229
	45	5.0	1.74–1.87	3.96–4.05	1.101–1.176
	45	4.0	1.82–1.97	4.25–4.36	1.125–1.203
	45	3.0	1.92–2.07	4.59–4.69	1.155–1.236

Experimental data are plotted against predicted data as demonstrated in Fig. 16a–c. It was found that the predicted Nusselt number, friction factor and thermo-hydraulic performance data agreed well with the experimental data. A summary of experimental results for Nu , f and thermo-hydraulic performance are given in Tables 2, 3 and 4.

6 Conclusions

The experimental results of heat transfer enhancement, friction factor and thermo-hydraulic performance using TiO_2 -water nanofluids under turbulent flow ($4000 \leq Re \leq 18,000$) in dimpled tubes with a TT inserts are presented. The effect of following parameters are reported: (1) the dimple angles of the dimpled tubes, $\theta = 0, 15, 30$ and 45° , (2) twist ratio of twisted tapes, $y/W = 3.0, 4.0$ and 5.0 , and (3) TiO_2 -water nanofluid concentrations, $\phi = 0.05, 0.1$ and 0.15 vol.\% .

- The dimpled tube with TT inserts consistently yielded higher heat transfer enhancement and caused higher friction factor than those of the dimpled tube or the plain tube alone.
- The dimpled tubes with the largest dimple angle, 45° , provided higher thermo-hydraulic performance than those at $0, 15$ and 30° by 1.5, 0.9 and 0.4%, respectively. The heat transfer rate at $\theta = 45^\circ$ was found to be higher than for dimple angles of $0, 15$ and 30° by 2.6, 1.6 and 0.7%, since the rougher dimples cause stronger turbulence than the smoother ones.
- For dimpled tubes with TT inserts, the heat transfer rate as well as pressure loss increased as y/W decreased. Over the entire range of parameters investigated, the heat transfer rates of dimpled tube with TT inserts at $y/W = 3.0, 4.0$ and

Table 4 Summary of experimental results for dimpled tube with twisted tape inserts at various nanofluid concentrations

Details	y/W	ϕ (vol.%)	Nu_E/Nu_0	f_E/f_0	η
Dimpled tube ($\theta = 45^\circ$)	5.0	0.05	1.75–1.88	3.98–4.07	1.102–1.177
	5.0	0.10	1.76–1.89	4.01–4.09	1.106–1.182
	5.0	0.15	1.76–1.91	4.02–4.11	1.110–1.189
	4.0	0.05	1.83–1.98	4.27–4.38	1.128–1.209
	4.0	0.10	1.84–1.99	4.29–4.41	1.131–1.211
	4.0	0.15	1.85–1.99	4.31–4.42	1.134–1.214
	3.0	0.05	1.92–2.08	4.61–4.71	1.157–1.241
	3.0	0.10	1.94–2.10	4.63–4.75	1.162–1.247
	3.0	0.15	1.95–2.12	4.66–4.78	1.167–1.258

5.0 were higher than those of the dimpled tube alone by 46.5, 39.2 and 32.7%, corresponding to higher thermo-hydraulic performances of 16.3, 13.1 and 10.6%, respectively.

- Over the investigated range, the highest thermo-hydraulic performance of 1.258 was achieved by using the nanofluid with $\phi = 0.15$ vol.% in the dimple angled having the dimple angle of 45° , inserted with twisted tape possessing the twist ratio of 3.0.

References

- Kalinin EK, Dreitser GA, Paramonov NV, Myakochin AS, Tikhonov AI, Zakirov SG, Levin ES, Yanovsky LS (1991) Comprehensive study of heat transfer enhancement in tubular heat exchangers. *Exp Thermal Fluid Sci* 4:656–666
- Giovannini A, Ferries B, Lotado B (1991) Aerothermal performances of enhanced heat transfer tubes in transitional regime for compact heat exchangers: problems associated with dimensioning criteria. *Entropie Seminar* no 9, pp 93–98
- Vicente PG, García A, Viedma A (2002) Heat transfer and pressure drop for low Reynolds turbulent flow in helically dimpled tubes. *Int J Heat Mass Tran* 45:543–553
- Kovalenko GV, Khalatov AA (2003) Fluid flow and heat transfer features at a cross-flow of dimpled tubes in a confined space. American Society of Mechanical Engineers, International Gas Turbine Institute, Turbo Expo (Publication) IGTI 5 B, pp 945–954
- Thianpong C, Eiamsa-ard P, Wongcharee K, Eiamsa-ard S (2009) Compound heat transfer enhancement of a dimpled tube with a twisted tape swirl generator. *Int Commun Heat Mass* 36:698–704
- Chudnovsky Y, Kurek HS, Kozlov A (2004) Dimpled tube technology for heat transfer enhancement in chemical industry process heaters. *Proceedings - natural gas technologies II: ingenuity and innovation*
- Balunov BF, Gotovskii MA, Permyakov VA, Permyakov KV, Saikova EN, Sal'nikov VV (2008) Studying the thermal and hydraulic characteristics of a shell-and-tube water heater equipped with dimpled heat-transfer tubes to enhance heat transfer. *Therm Eng* 55:67–71
- Chen Q, He Z, Liu J, Zhu G (2014) Numerical simulation of convection heat transfer and pressure loss for the protrusions in the dimpled tube. *Combust Sci Technol* 20:21–25
- Eiamsa-ard S, Wongcharee K, Eiamsa-ard P, Chuwattanakul V (2015) Heat transfer enhancement of turbulent flow through dimpled tubes fitted with twisted tapes. *International conference on power engineering (ICOPE 2015)*, Japan
- Suresh S, Chandrasekar M, Selvakumar P (2012) Experimental studies on heat transfer and friction factor characteristics of CuO/water nanofluid under laminar flow in a helically dimpled tube. *Heat Mass Transfer* 48:683–694
- Chen J, Müller-Steinhagen H, Duffy GG (2001) Heat transfer enhancement in dimpled tubes. *Appl Therm Eng* 21:535–547
- Wang Y, He YL, Lei YG, Li R (2009) Heat transfer and friction characteristics for turbulent flow of dimpled tubes. *Chem Eng Technol* 32:956–963
- Wang Y, He YL, Lei YG, Zhang J (2010) Heat transfer and hydrodynamics analysis of a novel dimpled tube. *Exp Thermal Fluid Sci* 34:1273–1281
- García A, Solano JP, Vicente PG, Viedma A (2012) The influence of artificial roughness shape on heat transfer enhancement: corrugated tubes, dimpled tubes and wire coils. *Appl Therm Eng* 35:196–201
- Kim NH (2015) Single-phase pressure drop and heat transfer measurements of turbulent flow inside helically dimpled tubes. *J Enhanc Heat Transf* 22:345–363
- Li M, Khan TS, Al-Hajri E, Ayub ZH (2016) Single phase heat transfer and pressure drop analysis of a dimpled enhanced tube. *Appl Therm Eng* 101:38–46
- Li BD, Liu P, Zheng MB, Liu ZC, Liu W (2016) Numerical simulation of helically dimpled tubes for convection heat transfer and pressure drop. *Kung Cheng je Wu Li Hsueh Pao. J Eng Thermophys Rus* 37:1261–1267
- Sarmadian A, Shafae M, Mashouf H, Mohseni SG (2017) Condensation heat transfer and pressure drop characteristics of R-600a in horizontal smooth and helically dimpled tubes. *Exp Thermal Fluid Sci* 86:54–62
- Kumar A, Maithani R, Suri ARS (2017) Numerical and experimental investigation of enhancement of heat transfer in dimpled rib heat exchanger tube. *Heat Mass Transfer* 53:3501–3516
- Ganjbakhsh N, Alikhani S, Behzadmehr A (2018) Numerical study of the effects of surface roughness on the mixed convection heat transfer of a laminar flow inside a horizontal curved dimpled tube. *Heat Mass Transfer* <https://doi.org/10.1007/s00231-018-2502-4>
- Xie S, Liang Z, Zhang L, Wang Y (2018) A numerical study on heat transfer enhancement and flow structure in enhanced tube with cross ellipsoidal dimples. *Int J Heat Mass Tran* 125:434–444
- Xie S, Liang Z, Zhang L, Wang Y, Ding H, Zhang J (2018) Numerical investigation on heat transfer performance and flow

- characteristics in enhanced tube with dimples and protrusions. *Int J Heat Mass Tran* 122:602–613
23. Xie S, Liang Z, Zhang J, Zhang L, Wang Y, Ding H (2019) Numerical investigation on flow and heat transfer in dimpled tube with teardrop dimples. *Int J Heat Mass Tran* 131:713–723
 24. Aroonrat K, Wongwises S (2019) Experimental investigation of condensation heat transfer and pressure drop of R-134a flowing inside dimpled tubes with different dimpled depths. *Int J Heat Mass Tran* 128:783–793
 25. Kumar S, Kothiyal AD, Bisht MS, Kumar A (2017) Turbulent heat transfer and nanofluid flow in a protruded ribbed square passage. *Results Physics* 7:3603–3618
 26. Akyürek EF, Geliş K, Şahin B, Manay E (2018) Experimental analysis for heat transfer of nanofluid with wire coil turbulators in a concentric tube heat exchanger. *Results Physics* 9:376–389
 27. Suresh S, Chandrasekar M, Chandra Sekhar S (2011) Experimental studies on heat transfer and friction factor characteristics of CuO/water nanofluid under turbulent flow in a helically dimpled tube. *Exp Thermal Fluid Sci* 35:542–549
 28. Eiamsa-ard S, Wongcharee K (2018) Convective heat transfer enhancement using ag-water nanofluid in a micro-fin tube combined with non-uniform twisted tape. *Int J Mech Sci* 146-147:337–354
 29. Waghole DR, Warkhedkar RM, Kulkarni VS, Shrivastva RK (2016) Studies on heat transfer in flow of silver nanofluid through a straight tube with twisted tape inserts. *Heat Mass Transf* 52:309–313
 30. Hazbehian M, Maddah H, Mohammadiun H, Alizadeh M (2016) Experimental investigation of heat transfer augmentation inside double pipe heat exchanger equipped with reduced width twisted tapes inserts using polymeric nanofluid. *Heat Mass Transf* 52: 2515–2529
 31. Arunachalam U, Edwin M (2018) Experimental studies on laminar flow heat transfer in nanofluids flowing through a straight circular tube with and without V-cut twisted tape insert. *Heat Mass Transf* 54:673–683
 32. ANSI/ASME. Measurement uncertainty. PTC 19, 1–1985. Part I, 1986
 33. Kline SJ, McClintock FA (1953) Describing uncertainties in single sample experiments. *Mech Eng* 75:3–8
 34. Pak BC, Cho IY (1998) Hydrodynamic and heat transfer study of dispersed fluids with sub-micron metallic oxide particles. *Exp Heat Transfer* 11:151–170
 35. Xuan Y, Roetzel W (2000) Conceptions for heat transfer correlation of nanofluids. *Int J Heat Mass Tran* 43:3701–3707
 36. Dewan A, Mahanta P, Sumithra Raju K, Kumar PS (2004) Review of passive heat transfer augmentation techniques. *Proceedings of the Institution of Mechanical Engineers, Part A: Journal of Power and Energy* 218:509–527
 37. Yakut K, Ba S, Canbazoglu S (2004) Performance and flow-induced vibration characteristics for conical-ring turbulators. *Appl Energ* 79:65–76
 38. Incropera F, Dewitt D (1996) *Introduction to heat transfer*, 3rd edn. Wiley, New York

Publisher's note Springer Nature remains neutral with regard to jurisdictional claims in published maps and institutional affiliations.